

## Anisotropy and mantle flow in the Chile-Argentina subduction zone from shear wave splitting analysis

Megan L. Anderson,<sup>1</sup> George Zandt,<sup>1</sup> Enrique Triep,<sup>2</sup> Matthew Fouch,<sup>3</sup> and Susan Beck<sup>1</sup>

Received 3 July 2004; revised 25 October 2004; accepted 3 November 2004; published 10 December 2004.

[1] We examine shear wave splitting in teleseismic phases to observe seismic anisotropy in the South American subduction zone. Data is from the CHARGE network, which traversed Chile and western Argentina across two transects between 30°S and 36°S. Beneath the southern and northwestern parts of the network, fast polarization direction ( $\varphi$ ) is consistently trench-parallel, while in the northeast  $\varphi$  is trench-normal; the transition between these two zones is gradual. We infer that anisotropy sampled by teleseismic phases is localized within or below the subducting slab. We explain our observations with a model in which eastward, Nazca-entrained asthenospheric flow is deflected by retrograde motion of the subducting Nazca plate. Resulting southward flow through this area produces N-S  $\varphi$  observed in the south and northwest; E-W  $\varphi$  result from interaction of this flow with the local slab geometry producing eastward mantle flow under the actively flattening part of the slab. **INDEX TERMS:** 7203 Seismology: Body wave propagation; 7218 Seismology: Lithosphere and upper mantle; 8123 Tectonophysics: Dynamics, seismotectonics; 8150 Tectonophysics: Plate boundary—general (3040); 9360 Information Related to Geographic Region: South America. **Citation:** Anderson, M. L., G. Zandt, E. Triep, M. Fouch, and S. Beck (2004), Anisotropy and mantle flow in the Chile-Argentina subduction zone from shear wave splitting analysis, *Geophys. Res. Lett.*, 31, L23608, doi:10.1029/2004GL020906.

### 1. Introduction

[2] At subduction zones there is close interaction of the ductile mantle and more rigid subducting slabs; therefore they are good places to test models of mantle flow using geophysical data. In this study, we characterize seismic anisotropy through observation of shear wave splitting in a part of the South American subduction zone in Chile and Argentina between 30°S and 36°S (Figure 1) and interpret it in terms of mantle flow. We assume that olivine deforming under the conditions of dislocation creep in the upper mantle will produce hexagonal type seismic anisotropy with a horizontal fast axis oriented in the direction of maximum strain [Zhang and Karato, 1995]. Recent studies have shown that upper mantle anisotropy may be significantly

more complex than this [Holtzman *et al.*, 2003; Mehl *et al.*, 2003], especially in the presence of water [Jung and Karato, 2001; Mizukami *et al.*, 2004]; we utilize the simpler assumption because our results indicate that the largest source of anisotropy in this region comes from within and below the slab (see discussion below), where significant quantities of water or melt are not likely to be present.

[3] Recent studies suggest that mantle is flowing parallel to the strike of the trench in some subduction zones both within the wedge [Fouch and Fischer, 1996; Mehl *et al.*, 2003; Smith *et al.*, 2001; Yang *et al.*, 1995] and below the slab [Peyton *et al.*, 2001; Russo and Silver, 1994]. The wedge observations contradict classic corner flow models which predict that mantle flow in subduction zones should be coupled to the plates involved and therefore should move in the same direction as the subducting plate and/or overriding plate [Buttles and Olson, 1998; Hall *et al.*, 2000; Kincaid and Sacks, 1997; Ribe, 1989]. Trench-parallel flow below the slab also contradicts these largely two-dimensional models, which assume strain in the asthenosphere below the subducting slab is parallel to relative plate motion (RPM) of the subducting plate with respect to the overriding plate. Instead, a combination of factors could influence below-slab anisotropy, including absolute plate motion (APM), lower mantle flow, retrograde trench/slab motion and local slab geometry. Here we present data that supports trench-parallel mantle flow below the subducting slab in the Chile-Argentina subduction zone. In addition, this region is an excellent natural laboratory for studying the effect of local slab geometry on mantle flow; between 33°S and 36°S the subducting Nazca slab has a uniform dip of approximately 30° but between 30° and 33°, the slab flattens at a depth of ~100 km and extends east from the trench at this depth for almost 300 km before it continues dipping into the mantle [Cahill and Isacks, 1992] (Figure 1). Our results support a strong spatial connection of mantle flow direction to the geometry of the subducting slab.

### 2. Shear Wave Splitting Analysis and Results

[4] We utilized the shear wave splitting method of Silver and Chan [1991] on SKS, SKKS, and PKS arrivals from earthquakes between 85° and 140° away from the Chile Argentina Geophysical Experiment (CHARGE) broadband network (Figure 2) to constrain the best-fitting fast polarization direction ( $\varphi$ ) and splitting delay time between fast and slow shear waves ( $\delta t$ ) for each station in the network. In addition, we analyzed data from GEOSCOPE station PEL in Chile (Figure 1). We assessed the quality of our results using both quantitative and qualitative factors, and used the quality of individual measurements to calculate a weighted average  $\varphi$  and  $\delta t$  for each station (Figure 1). See the

<sup>1</sup>Department of Geosciences, University of Arizona, Tucson, Arizona, USA.

<sup>2</sup>Department of Geophysics and Astronomy, National University of San Juan, San Juan, Argentina.

<sup>3</sup>Department of Geological Sciences, Arizona State University, Tempe, Arizona, USA.

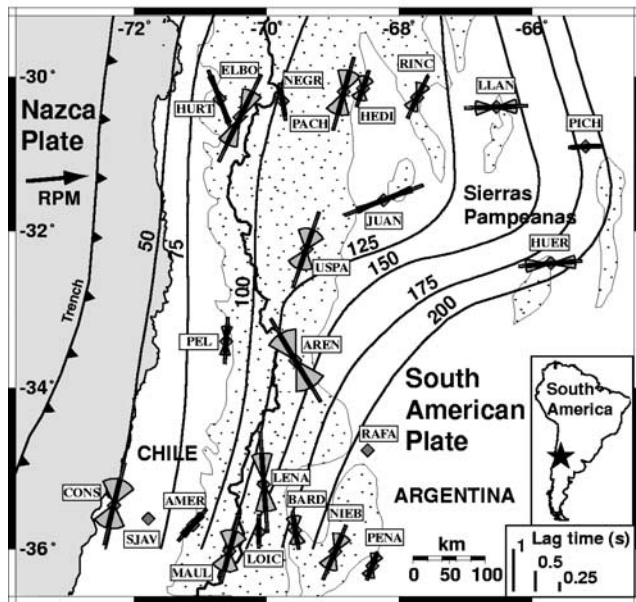


**Figure 1.** Average fast axis orientation ( $\varphi$ ) and lag time ( $\delta t$ ; refer to scale) for each station (grey diamonds) of the CHARGE network and GEOSCOPE station PEL. Index map shows location relative to South America. Errors, or the standard deviation on the average  $\varphi$  for each station are indicated by “bow-ties” and where absent, are smaller than the width of the fast axis marker. Error, also the standard deviation, of  $\delta t$  are indicated by the light grey bars in the azimuth of  $\varphi$ ; only the error in the positive direction is shown. Contours of the depth of the subducting slab are labeled in kilometers and are from Cahill and Isacks [1992]. Mountains of the Andes (elevations > 450 m) are indicated by the hachured areas. Direction of plate motion (RPM) of the Nazca plate relative to a fixed South America is indicated by the arrow.

auxiliary material<sup>1</sup> for details on the waveform analysis, resulting measurements, error assessment, and calculation of weighted averages.

[5] The magnitude of  $\delta t$  for all measurements varies between 0.3 and 3.3 s with an average of 0.95 s. Errors for individual measurements as well as the standard deviation of measurements at each station are similar and average  $\sim 0.5$  s for  $\delta t$  and  $\sim 25$  degrees for  $\varphi$ . The data at some stations show considerable variation (see the auxiliary material and Figure 1), which indicates that the source of anisotropy at some stations is complex, either due to variation of  $\varphi$  and  $\delta t$  with depth or a dipping fast axis. Even with these complexities, the azimuths of the average fast direction vary quite uniformly across the network (Figure 1). Under the southern and northwestern parts of the network,  $\varphi$  is consistently N-S with  $\delta t \sim 0.9$  s, while in the northeastern part of the network  $\varphi$  is consistently E-W with  $\delta t \sim 1.0$  s. The fast axis is oriented northeast, parallel to slab contours, adjacent to the slab dip transition at two stations in the center of the network (USPA and JUAN in Figure 1), indicating a spatial correlation between  $\varphi$  and

slab geometry. In addition,  $\delta t$  for these stations with AREN and PEL averages 1.1 s, a little higher than the other stations, which may indicate higher strain.

### 3. Anisotropy and Mantle Strain

[6] In order to interpret the shear wave splitting in terms of anisotropy, we need to first constrain the depth of the anisotropic layer(s). Anisotropy exists in the lowermost mantle beneath the central Pacific Ocean [e.g., Fouch et al., 2001; Garnero and Lay, 1997; Ritsema et al., 1997], but the geometry of the anisotropy is interpreted to produce a limited effect on nearly vertically-propagating core phases [Kaneshima and Silver, 1992]. In addition, we believe that the source of anisotropy is in the upper mantle beneath the CHARGE array because of the heterogeneities in  $\varphi$  observed across our network for the same event and the agreement of  $\varphi$  and  $\delta t$  for different events at many stations. We will separately consider possible sources of anisotropy from the crust and the mantle wedge, the slab itself, and the asthenosphere below the slab, which could all potentially affect the teleseismic measurements.

[7] Transverse components of receiver functions calculated with the CHARGE data show clear evidence for upper-plate crustal anisotropy in the northwestern part of the network above the flat slab area [Gilbert et al., 2003]. Results from the southern and northeastern portion of the network suggest that crustal anisotropy is weak or absent. The magnitude and direction of the anisotropy is not yet resolved with this data, however, the few shear wave-splitting measurements we have obtained from crustal events indicates negligible crustal anisotropy. In addition, preliminary shear wave splitting for local S waves from earthquakes located at  $\sim 100$  km depth within the flat subducting slab show  $\delta t$  on the order of 0.1 s [Anderson et al., 2003, also unpublished data]. The fast polarization direction of these results mimics the resolved  $\varphi$  for our teleseismic results. While we acknowledge that the magnitude of  $\delta t$  in the southeastern part of the network is likely to be larger where the mantle wedge is thicker, we assume that most of the overriding crust and wedge combined only

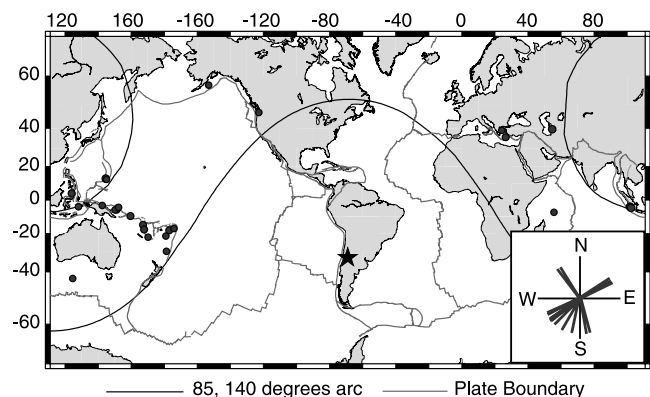


**Figure 2.** Teleseismic earthquakes used in this study. Star indicates the location of the CHARGE network and lines indicate distances of 85 and 140 degrees of arc away from this location. Earthquakes we investigated for this study are shown by the dark grey dots (inset shows distribution of backazimuths for these earthquakes).

<sup>1</sup>Auxiliary material is available at <ftp://ftp.agu.org/apend/gl/2004GL020906>.

produce  $\sim 0.1$  s of the total  $\delta t$  of the teleseismic results; this implies that the bulk of the anisotropy sampled by teleseismic phases originates from within or below the slab.

[8] Constraining the depth and magnitude of anisotropy within and/or below the subducting slab is complex. However, we can make some inferences based on some simple calculations and our knowledge of anisotropy along the East Pacific Rise (EPR). First, if we assume a homogeneous 3% anisotropy, we can use the formulation developed by *Silver and Chan* [1991] to estimate a thickness of anisotropic mantle resulting from the observed range of teleseismic  $\delta t$  for the CHARGE network. After correcting for the estimated 0.1 s of splitting due to the mantle wedge and overriding crust, we estimate a layer 75–200 km thick within and below the subducting slab. Simple thermal models for 40–50 Ma subducted oceanic lithosphere predict a  $900^\circ$  isotherm, the depth above which lithosphere will retain fossil anisotropy [*Savage*, 1999], at about 40–50 km below the top of the subducting slab [*Gutscher et al.*, 2000]. Comparing this value to the thickness of anisotropic mantle calculated above, it is likely that both within- and below-slab sources of anisotropy exist at most stations.

[9] Second, we have some knowledge of fossil anisotropy that is likely to exist within the subducting Nazca plate. In the case of the South American subduction zone, spreading processes at the EPR would generate this anisotropy, and shear wave splitting studies have shown consistent, E-W oriented  $\varphi$  with  $\delta t$  of 1.0 s just off the Nazca side of the ridge axis [*Wolfe and Solomon*, 1998]. The depth is not well constrained and likely includes components in both the lithosphere and asthenosphere. Again, an estimation using 3% anisotropy within a 40–50 km thick layer of anisotropic lithosphere within the subducting plate results in a  $\delta t$  of 0.3 s. The ridge axis azimuth and Nazca plate motion vector have changed little over the last 40 Ma [*Pardo-Casas and Molnar*, 1987], therefore we expect an E-W orientation for this fossil anisotropy.

[10] There are few, if any independent sources of information on the direction of sub-slab asthenospheric flow and resulting anisotropy. If the mantle strain is dominantly influenced by RPM of the Nazca plate with respect to South America (Figure 1) and eastward mantle flow from the EPR, the resulting anisotropic fast axis would be oriented E-W [*Demets et al.*, 1994; *Norabuena et al.*, 1999]. Thus, models for possible sources of within- and below-slab asthenospheric anisotropy due to known spreading ridge processes or plate motion give an expected anisotropic fast direction of E-W, while many of the observed  $\varphi$  resolved from CHARGE data are N-S. This observation could be explained by a combination of remaining influences: unresolved lower mantle flow, APM for the Nazca plate, retrograde trench motion, and/or local slab configuration. It is not within the scope of this study to look at the first two factors, therefore we will investigate the plausibility of a simple model involving only RPM, retrograde trench motion, and the local slab geometry.

#### 4. Mantle Flow and Slab Geometry

[11] *Russo and Silver* [1994] suggested that below-slab, trench parallel anisotropy observed along other parts of the South American subduction zone could be explained by

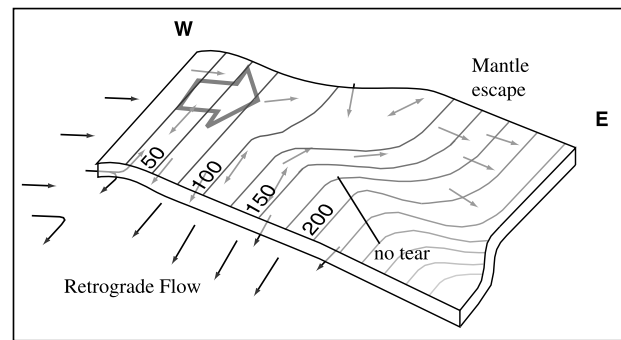


**Figure 3.** Schematic representation of asthenospheric mantle flow beneath the subducting slab interpreted from the fast polarization directions from Figure 1. Large arrow indicates direction of Nazca plate movement. Small arrows indicate local below-slab asthenospheric flow from our interpretation of teleseismic shear wave splitting. In this model, mantle flowing eastward entrained by the Nazca plate encounters resistance due to retrograde motion of the subducting slab and is diverted into a southward directed flow in the southern part of our study area and continues flowing eastward in the northeastern part of our study area. We indicate a continuous Nazca plate (see zone labeled “no tear”) due to the slab contour-parallel direction of anisotropy along the bend of the slab.

retrograde motion of the slab, due to the westward movement of the South American plate, paired with a barrier to flow at some depth (perhaps the 410 km discontinuity). This would cause a N or S component of below-slab asthenospheric flow allowing for the escape of mantle around the northern or southern limits of the Nazca plate from the Nazca-side mantle reservoir behind the retreating slab into the Atlantic-side mantle reservoir in front of the slab. This mantle flow model is generally consistent with observations in other parts of the South American subduction zone that exhibit trench-parallel below-slab fast polarization directions [*Bock et al.*, 1998; *Polet et al.*, 2000; *Russo and Silver*, 1994]. *Peyton et al.* [2001] used a similar model to explain trench-parallel anisotropy in the Kamchatka subduction zone. *Buttles and Olson* [1998] showed that the response of a viscous fluid to retrograde motion of a Plexiglas “subducting plate” will create trench parallel flow below the plate.

[12] We may be able to explain our observed splitting parameters by imposing the local slab geometry on this flow model, which predicts a southward mantle flow in our study area (Figure 3). The flattening subducting Nazca plate under the Sierras Pampeanas (Figure 1) creates space underneath to accommodate eastward mantle flow, therefore we would expect to observe E-W fast directions in the northeastern (actively flattening) part of our study area. Under the southern part of the study area there is no such space, therefore mantle continues to flow south. At the transition, flow predicted by the fast axis is oriented parallel to the contours of the subducting slab; our interpretation is that mantle strain in this zone is guided by the curve of a continuous slab. If there were a tear in the plate, we would expect N-S or NW-SE flow in this zone due to mantle escaping from below the slab through the tear similar to that seen in New Zealand [*Matcham et al.*, 2000]. The variability

ity in fast direction observed at some stations in the context of this model would then be due to complications introduced by the small component of upper-plate crustal and mantle wedge anisotropy and anisotropy within the subducting slab lithosphere.

[13] Our observations suggest that asthenospheric deformation in a subduction zone can be largely guided by the geometry of the subducting lithosphere. This conclusion could be further tested with numerical or analog models in order to confirm the mantle dynamics and boundary conditions inherent in our model or suggest other alternatives. Further analysis of the crustal components of anisotropy, continuing analysis of above/below slab mantle components, and modeling of the teleseismic splitting with multiple anisotropic layers will be necessary to develop a more finely resolved picture of anisotropy on all levels in the Chile-Argentina subduction zone. With increasing resolution from local networks and focused high-resolution seismometer deployments, the details of these potential local-scale effects can be more directly considered as parts of subduction zone mantle flow models.

[14] **Acknowledgments.** The CHARGE deployment is supported by NSF Grant #EAR9811870. The first author was also supported under a National Science Foundation Graduate Research Fellowship. CHARGE data were acquired with the help of the PASSCAL program and this data, as well as GEOSCOPE data are managed by IRIS. We would like to thank all members of the CHARGE Working Group, INPRES, and the National University of San Juan for their labor in acquiring data. Thanks to Cecily Wolfe for maintaining and providing access to the shear wave splitting analysis code, and to Martha Savage, Paul Silver, and Ray Russo for sharing their expertise on shear wave splitting analysis and calculating two-layer anisotropic models.

## References

- Anderson, M. L., G. Zandt, M. J. Fouch, and E. Triep (2003), Anisotropy in the Chile-Argentina flat slab subduction zone, South America, *Eos Trans. AGU*, 84(46), Fall Meet. Suppl., Abstract S41A-06.
- Bock, G., R. Kind, A. Rudloff, and G. Asch (1998), Shear wave anisotropy in the upper mantle beneath the Nazca plate in northern Chile, *J. Geophys. Res.*, 103, 24,333–24,345.
- Buttles, J., and P. Olson (1998), A laboratory model of subduction zone anisotropy, *Earth Planet. Sci. Lett.*, 164, 245–262.
- Cahill, T., and B. L. Isacks (1992), Seismicity and shape of the subducted Nazca plate, *J. Geophys. Res.*, 97, 17,503–17,529.
- Demets, C., R. G. Gordon, D. F. Argus, and S. Stein (1994), Effect of recent revisions to the geomagnetic reversal time-scale on estimates of current plate motions, *Geophys. Res. Lett.*, 21, 2191–2194.
- Fouch, M. J., and K. M. Fischer (1996), Mantle anisotropy beneath north-west Pacific subduction zones, *J. Geophys. Res.*, 101, 15,987–16,002.
- Fouch, M. J., K. M. Fischer, and M. E. Wyssession (2001), Lowermost mantle anisotropy beneath the Pacific: Imaging the source of the Hawaiian plume, *Earth Planet. Sci. Lett.*, 190, 167–180.
- Garnero, E. J., and T. Lay (1997), Lateral variations in lowermost mantle shear wave anisotropy beneath the north Pacific and Alaska, *J. Geophys. Res.*, 102, 8121–8135.
- Gilbert, H. J., S. Beck, G. Zandt, and the CHARGE Working Group (2003), Crustal structure of central Chile and Argentina, *Eos Trans. AGU*, 84(46), Fall Meet. Suppl., Abstract S41F-05.
- Gutscher, M. A., R. Maury, J. P. Eissen, and E. Bourdon (2000), Can slab melting be caused by flat subduction?, *Geology*, 28, 535–538.
- Hall, C. E., K. M. Fischer, E. M. Parmentier, and D. K. Blackman (2000), The influence of plate motions on three-dimensional back arc mantle flow and shear wave, *J. Geophys. Res.*, 105, 28,009–28,033.
- Holtzman, B. K., D. L. Kohlstedt, M. E. Zimmerman, F. Heidelbach, T. Hiraga, and J. Hustoft (2003), Melt segregation and strain partitioning: Implications for seismic anisotropy and mantle flow, *Science*, 301, 1227–1230.
- Jung, H., and S. Karato (2001), Water-induced fabric transitions in olivine, *Science*, 293, 1460–1463.
- Kaneshima, S., and P. G. Silver (1992), A search for source side mantle anisotropy, *Geophys. Res. Lett.*, 19, 1049–1052.
- Kincaid, C., and I. S. Sacks (1997), Thermal and dynamical evolution of the upper mantle in subduction zones, *J. Geophys. Res.*, 102, 12,295–12,315.
- Matcham, I., M. K. Savage, and K. R. Gledhill (2000), Distribution of seismic anisotropy in the subduction zone beneath the Wellington region, New Zealand, *Geophys. J. Int.*, 140, 1–10.
- Mehl, L., B. R. Hacker, G. Hirth, and P. B. Kelemen (2003), Arc-parallel flow within the mantle wedge: Evidence from the accreted Talkeetna arc, south central Alaska, *J. Geophys. Res.*, 108(B8), 2375, doi:10.1029/2002JB002233.
- Mizukami, T., S. R. Wallis, and J. Yamamoto (2004), Natural examples of olivine lattice preferred orientation patterns with a flow normal a-axis maximum, *Nature*, 427, 432–436.
- Norabuena, E. O., T. H. Dixon, S. Stein, and C. G. A. Harrison (1999), Decelerating Nazca-South America and Nazca-Pacific Plate motions, *Geophys. Res. Lett.*, 26, 3405–3408.
- Pardo-Casas, F., and P. Molnar (1987), Relative motion of the Nazca (Farallon) and South-American Plates since Late Cretaceous time, *Tectonics*, 6, 233–248.
- Peyton, V., V. Levin, J. Park, M. Brandon, J. Lees, E. Gordeev, and A. Ozerov (2001), Mantle flow at a slab edge: Seismic anisotropy in the Kamchatka region, *Geophys. Res. Lett.*, 28, 379–382.
- Polet, J., P. G. Silver, S. Beck, T. Wallace, G. Zandt, S. Ruppert, R. Kind, and A. Rudloff (2000), Shear wave anisotropy beneath the Andes from the BANJO, SEDA, and PISCO experiments, *J. Geophys. Res.*, 105, 6287–6304.
- Ribe, N. M. (1989), Seismic anisotropy and mantle flow, *J. Geophys. Res.*, 94, 4213–4223.
- Ritsema, J., E. Garnero, and T. Lay (1997), A strongly negative shear velocity gradient and lateral variability in the lowermost mantle beneath the Pacific, *J. Geophys. Res.*, 102, 20,395–20,411.
- Russo, R. M., and P. G. Silver (1994), Trench-parallel flow beneath the Nazca plate from seismic anisotropy, *Science*, 263, 1105–1111.
- Savage, M. K. (1999), Seismic anisotropy and mantle deformation: What have we learned from shear wave splitting?, *Rev. Geophys.*, 37, 65–106.
- Silver, P. G., and W. W. Chan (1991), Shear wave splitting and subcontinental mantle deformation, *J. Geophys. Res.*, 96, 16,429–16,454.
- Smith, G. P., D. A. Wiens, K. M. Fischer, L. M. Dorman, S. C. Webb, and J. A. Hildebrand (2001), A complex pattern of mantle flow in the Lau backarc, *Science*, 292, 713–716.
- Wolfe, C. J., and S. C. Solomon (1998), Shear-wave splitting and implications for mantle flow beneath the MELT region of the East Pacific Rise, *Science*, 280, 1230–1232.
- Yang, X. P., K. M. Fischer, and G. A. Abers (1995), Seismic anisotropy beneath the Shumagin Islands segment of the Aleutian-Alaska subduction zone, *J. Geophys. Res.*, 100, 18,165–18,177.
- Zhang, S. Q., and S. Karato (1995), Lattice preferred orientation of olivine aggregates deformed in simple shear, *Nature*, 375, 774–777.

M. L. Anderson, S. Beck, and G. Zandt, Department of Geosciences, University of Arizona, 1040 E. 4th Street, Tucson, AZ 85716, USA. (anderson@geo.arizona.edu)

M. Fouch, Department of Geological Sciences, Arizona State University, Box 871404, Tempe, AZ 85287, USA.

E. Triep, Department of Geophysics and Astronomy, National University of San Juan, Meglioli 1160-Sur, Rivadavia, San Juan, SJ 56400, Argentina.